Variational Methods for Manifold-valued Image Processing[a]

Ronny Bergmann

Technische Universität Chemnitz

Seminar “Theory and Algorithms in Data Science”, Alan Turing Institute,

London, September 3rd, 2018.

[a] supported by DFG Grant BE 5888/2-1

Contents

Introduction

Manifold-valued Images

New data acquisition modalities lead to non-Euclidean range

- Interferometric synthetic aperture radar (InSAR)
- Surface normals, GPS data, wind, flow,...
- Diffusion tensors in magnetic resonance imaging (DT-MRI), covariance matrices
- Electron backscattered diffraction (EBSD)

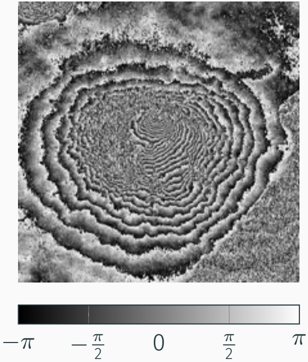

InSAR-Data of Mt. Vesuvius

[Rocca, Prati, Guarnieri 1997]

phase-valued data, $\mathcal{M} = \mathbb{S}^1$

Manifold-valued Images

New data acquisition modalities lead to non-Euclidean range

- Interferometric synthetic aperture radar (InSAR)
- Surface normals, GPS data, wind, flow,...
- Diffusion tensors in magnetic resonance imaging (DT-MRI), covariance matrices
- Electron backscattered diffraction (EBSD)

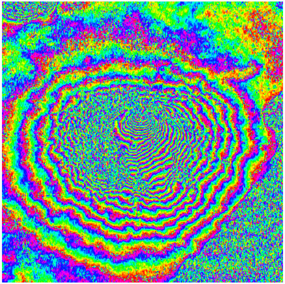

InSAR-Data of Mt. Vesuvius

[Rocca, Prati, Guarnieri 1997]

phase-valued data, $\mathcal{M} = \mathbb{S}^1$

Manifold-valued Images

New data acquisition modalities lead to non-Euclidean range

- Interferometric synthetic aperture radar (InSAR)
- Surface normals, GPS data, wind, flow,...
- Diffusion tensors in magnetic resonance imaging (DT-MRI), covariance matrices
- Electron backscattered diffraction (EBSD)

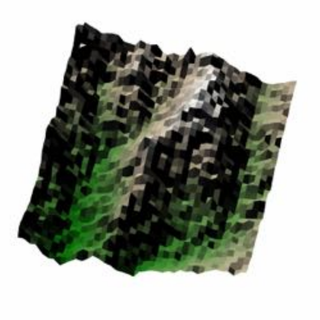

National elevation dataset
[Gesch, Evans, Mauck, 2009]

directional data, $\mathcal{M} = \mathbb{S}^2$

Manifold-valued Images

New data acquisition modalities lead to non-Euclidean range

- Interferometric synthetic aperture radar (InSAR)
- Surface normals, GPS data, wind, flow,...
- Diffusion tensors in magnetic resonance imaging (DT-MRI), covariance matrices
- Electron backscattered diffraction (EBSD)

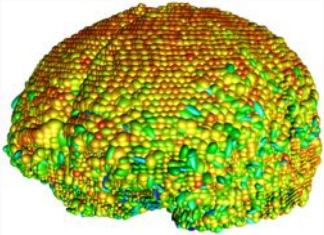

diffusion tensors in human brain from the Camino dataset
http://cmic.cs.ucl.ac.uk/camino

sym. pos. def. matrices, $\mathcal{M} = \mathrm{SPD}(3)$

Manifold-valued Images

New data acquisition modalities lead to non-Euclidean range

- Interferometric synthetic aperture radar (InSAR)
- Surface normals, GPS data, wind, flow,...
- Diffusion tensors in magnetic resonance imaging (DT-MRI), covariance matrices
- Electron backscattered diffraction (EBSD)

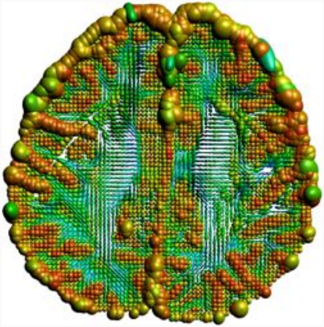

horizontal slice #28
from the Camino dataset
http://cmic.cs.ucl.ac.uk/camino

sym. pos. def. matrices, $\mathcal{M} = \mathrm{SPD}(3)$

Manifold-valued Images

New data acquisition modalities lead to non-Euclidean range

- Interferometric synthetic aperture radar (InSAR)
- Surface normals, GPS data, wind, flow,…
- Diffusion tensors in magnetic resonance imaging (DT-MRI), covariance matrices
- Electron backscattered diffraction (EBSD)

EBSD example from the MTEX toolbox
[Bachmann, Hielscher, since 2005]

Rotations (mod. symmetry),
$\mathcal{M} = \mathrm{SO}(3)(/\mathcal{S})$.

Manifold-valued Images

New data acquisition modalities lead to non-Euclidean range

- Interferometric synthetic aperture radar (InSAR)
- Surface normals, GPS data, wind, flow,…
- Diffusion tensors in magnetic resonance imaging (DT-MRI), covariance matrices
- Electron backscattered diffraction (EBSD)

Common properties

- Range of values is a Riemannian manifold
- Tasks from “classical” image processing, e.g.
    - denoising
    - inpainting
    - labeling
    - deblurring

(real-valued) Variational Methods

Setting. From $u_0 : \mathbb{R}^m \supset \Omega \to \mathbb{R}^n$ we observe $f \coloneqq Ku_0 + \eta$ with

- a linear operator K
- Gaussian white noise η

Task. Reconstruct u_0 from given data f.

Ansatz. Compute minimizer u^* of the variational model

$$\mathcal{E}(u) \coloneqq \mathcal{D}(u; f) + \alpha \mathcal{R}(u), \quad \alpha > 0,$$

with

- similarity or data fidelity term $\mathcal{D}(u; f) = \|Ku - f\|_{L_2}^2$
- reguilarizer $\mathcal{R}(u)$ containing a priori knowledge about u_0

Regularisers for Denoising ($K = \mathrm{Id}$)

Intuition. Smoothen f while keeping its main features

- Tichonov-Regulariser (H^1-Seminorm)
- first order derivative
- second order derivative
- combine first and second order derivatives

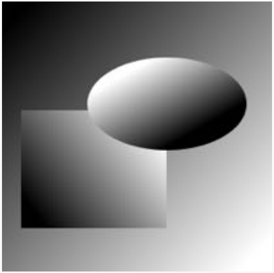

u_0.

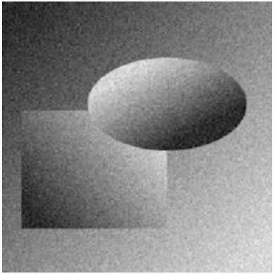

f.

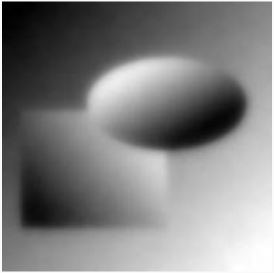

Tichonov.

images (adapted) from [Setzer, Steidl, Teuber, 2009]

Regularisers for Denoising ($K = \mathrm{Id}$)

Intuition. Smoothen f while keeping its main features

- Tichonov-Regulariser (H^1-Seminorm)
- first order derivative
- second order derivative
- combine first and second order derivatives

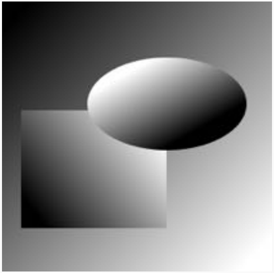

u_0.

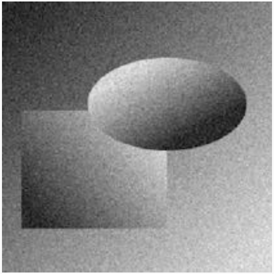

f.

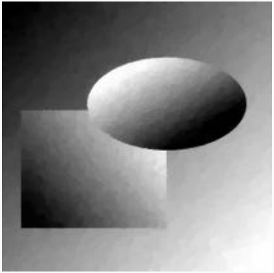

first order.

images (adapted) from [Setzer, Steidl, Teuber, 2009]

Regularisers for Denoising ($K = \mathrm{Id}$)

Intuition. Smoothen f while keeping its main features

- Tichonov-Regulariser (H^1-Seminorm)
- first order derivative
- second order derivative
- combine first and second order derivatives

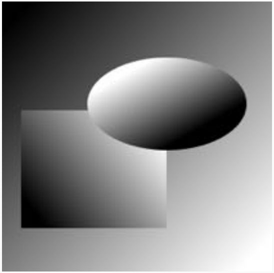

u_0.

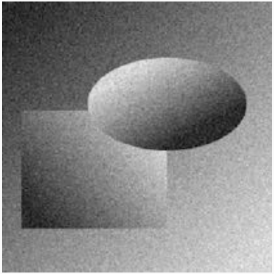

f.

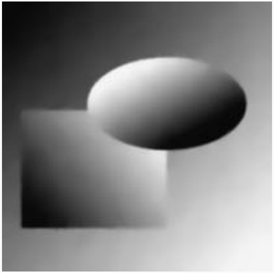

first plus second order.

images (adapted) from [Setzer, Steidl, Teuber, 2009]

Intuition. Smoothen f while keeping its main features

- Tichonov-Regulariser (H^1-Seminorm)
- first order derivative
- second order derivative
- combine first and second order derivatives

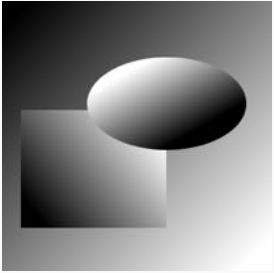

u_0.

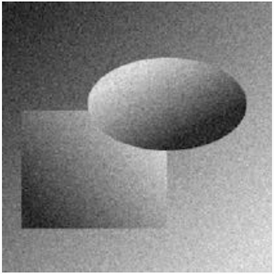

f.

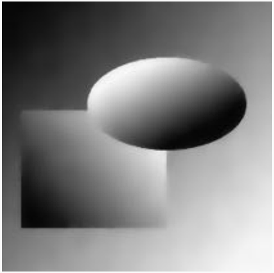

TGV.

images (adapted) from [Setzer, Steidl, Teuber, 2009]

Digital Images

For $\Omega \supset [1,N]\times[1,M]$ set $\mathcal{G} = \Omega \cap \mathbb{Z}^2 = \{1,\ldots,N\}\times\{1,\ldots,M\}$.
We define the (discrete) Total Variation (TV) by

$$\mathrm{TV}(u) = \|\nabla u\|_{2,1} = \sum_{(i,j)\in\mathcal{G}} \Big\| \Big((\nabla_x u)_{i,j} \quad (\nabla_y u)_{i,j} \Big)^{\mathrm{T}} \Big\|_2$$

with forward differences of $u\colon \mathcal{G} \to \mathbb{R}$ as

$$(\nabla_x u)_{i,j} = \begin{cases} u_{i+1,j} - u_{i,j} & \text{if } i < N, \\ 0 & \text{else,} \end{cases}$$

$$(\nabla_y u)_{i,j} = \begin{cases} u_{i,j+1} - u_{i,j} & \text{if } j < M, \\ 0 & \text{else.} \end{cases}$$

Digital Images

For $\Omega \supset [1, N] \times [1, M]$ set $\mathcal{G} = \Omega \cap \mathbb{Z}^2 = \{1, \ldots, N\} \times \{1, \ldots, M\}$.
We define the (discrete) Total Variation (TV) by

$$\mathrm{TV}(u) = \|\nabla u\|_{2,1} = \sum_{(i,j)\in\mathcal{G}} \left\| \Big((\nabla_x u)_{i,j} \quad (\nabla_y u)_{i,j} \Big)^{\mathrm{T}} \right\|_2$$

with forward differences of $u \colon \mathcal{G} \to \mathbb{R}$ as

$$(\nabla_x u)_{i,j} = \begin{cases} u_{i+1,j} - u_{i,j} & \text{if } i < N, \\ 0 & \text{else,} \end{cases}$$

$$(\nabla_y u)_{i,j} = \begin{cases} u_{i,j+1} - u_{i,j} & \text{if } j < M, \\ 0 & \text{else.} \end{cases}$$

With backward differences $\tilde{\nabla}_x u, \tilde{\nabla}_y u$: Second Order TV

$$\mathrm{TV}_2(u) = \|\nabla^2 u\|_{2,1}, \quad \nabla^2 = \Big(\tilde{\nabla}_x \nabla_x \quad \tfrac{1}{2}(\tilde{\nabla}_x \nabla_y + \tilde{\nabla}_y \nabla_x) \quad \tilde{\nabla}_y \nabla_y \Big)^{\mathrm{T}}.$$

Variational Models for Digital Images

Reconstruct $u_0\colon \mathcal{G} \to \mathbb{R}^n$ from measurements $f\colon \mathcal{G} \supset \mathcal{V} \to \mathbb{R}^n$

Ansatz. Compute minimizer u^* of the variational model

$$\mathcal{E}(u) \coloneqq \underbrace{\mathcal{D}(u;f)}_{\text{data fidelity}} + \underbrace{\alpha\,\mathcal{R}(u)}_{\text{regulariser}}, \qquad \alpha > 0.$$

- high dimensional, $\mathcal{E}\colon \mathbb{R}^{NMn} \to \mathbb{R}$
- not differentiable
- (often) convex

Reconstruct $u_0 \colon \mathcal{G} \to \mathbb{R}^n$ from measurements $f \colon \mathcal{G} \supset \mathcal{V} \to \mathbb{R}^n$

Ansatz. Compute minimizer u^* of the variational model

$$\mathcal{E}(u) := \underbrace{\mathcal{D}(u; f)}_{\text{data fidelity}} + \underbrace{\alpha\,\mathcal{R}(u)}_{\text{regulariser}}, \quad \alpha > 0.$$

- high dimensional, $\mathcal{E} \colon \mathbb{R}^{NMn} \to \mathbb{R}$
- not differentiable
- (often) convex

Example: TV regularizer model for a signal f

[Rudin, Osher, Fatemi, 1992]

$$\mathcal{E}(u) = \sum_{i=1}^{N} \|u_i - f_i\|^2 + \alpha \sum_{i=1}^{N-1} \|u_{i+1} - u_i\|$$

Variational Models for Digital Images

Reconstruct $u_0 \colon \mathcal{G} \to \mathbb{R}^n$ from measurements $f \colon \mathcal{G} \supset \mathcal{V} \to \mathbb{R}^n$

Ansatz. Compute minimizer u^* of the variational model

$$\mathcal{E}(u) \coloneqq \underbrace{\mathcal{D}(u; f)}_{\text{data fidelity}} + \underbrace{\alpha\, \mathcal{R}(u)}_{\text{regulariser}}, \quad \alpha > 0.$$

- high dimensional, $\mathcal{E} \colon \mathbb{R}^{NMn} \to \mathbb{R}$
- not differentiable
- (often) convex

Example: additive coupling model for a signal f

[Rudin, Osher, Fatemi, 1992]

$$\mathcal{E}(u) = \sum_{i=1}^{N} \|u_i - f_i\|^2 + \alpha \sum_{i=1}^{N-1} \|u_{i+1} - u_i\| + \beta \sum_{i=2}^{N-1} \|u_{i-1} - 2u_i + u_{i+1}\|$$

Variational Models for Digital Images

Reconstruct $u_0 \colon \mathcal{G} \to \mathbb{R}^n$ from measurements $f \colon \mathcal{G} \supset \mathcal{V} \to \mathbb{R}^n$

Ansatz. Compute minimizer u^* of the variational model

$$\mathcal{E}(u) \coloneqq \underbrace{\mathcal{D}(u;f)}_{\text{data fidelity}} + \underbrace{\alpha\,\mathcal{R}(u)}_{\text{regulariser}}, \qquad \alpha > 0.$$

- high dimensional, $\mathcal{E} \colon \mathbb{R}^{NMn} \to \mathbb{R}$
- not differentiable
- (often) convex

Today.

Variational models for images $f \colon \mathcal{V} \to \mathcal{M}$
with pixel values in a Riemannian manifold $\mathcal{M}$.

A d-dimensional Riemannian Manifold $\mathcal{M}$

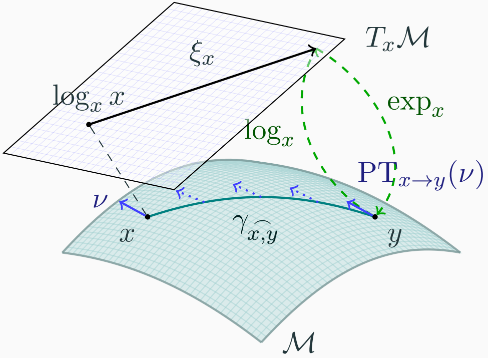

A d-dimensional Riemannian manifold can be informally defined as a set $\mathcal{M}$ covered with a 'suitable' collection of charts, that identify subsets of $\mathcal{M}$ with open subsets of $\mathbb{R}^d$ and a continously varying inner product on the tangential spaces.

[Absil, Mahony, Sepulchre, 2008]

A d-dimensional Riemannian Manifold $\mathcal{M}$

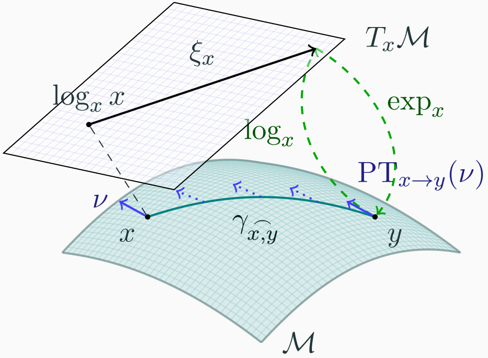

Geodesic $\gamma_{\widehat{x,y}}$ shortest connection (on $\mathcal{M}$) between $x, y \in \mathcal{M}$
Tangent space $\mathrm{T}_x\mathcal{M}$ at x, with inner product $\langle\cdot,\cdot\rangle_x$
Logarithmic map $\log_x y = \dot\gamma_{\widehat{x,y}}(0)$ "speed towards y"
Exponential map $\exp_x \xi_x = \gamma(1)$, where $\gamma(0) = x$, $\dot\gamma(0) = \xi_x$
Parallel transport $\mathrm{PT}_{x\to y}(\nu)$ of $\nu \in \mathrm{T}_x\mathcal{M}$ along $\gamma_{\widehat{x,y}}$

A Signal of Cyclic Data

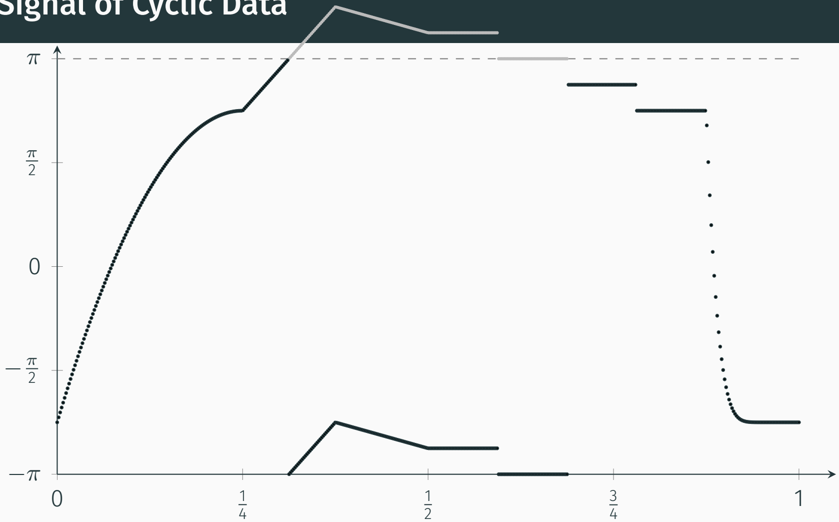

- A function $f\colon [0,1] \to \mathbb{S}^1$ is sampled $\Rightarrow f_o = (f_{o,i})_{i=1}^{500}$
- Data f stems from the gray plot via modulo
- Jumps $> \pi$ at $\frac{5}{16}$ and $\frac{11}{16}$ just from choice of representation

A Signal of Cyclic Data

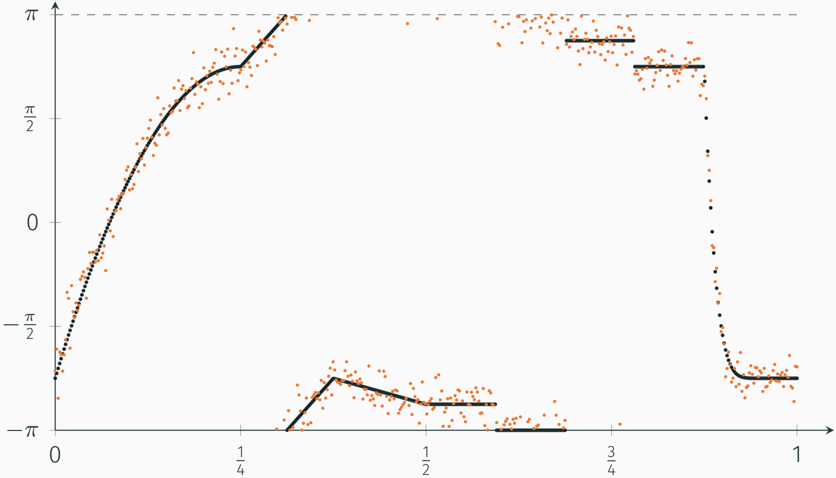

- A function $f\colon [0,1] \to \mathbb{S}^1$ is sampled $\Rightarrow f_o = (f_{o,i})_{i=1}^{500}$
- Noise: wrapped Gaussian, $\sigma = 0.2$
- noisy $f_n = (f_o + \eta)_{2\pi}$

A Signal of Cyclic Data

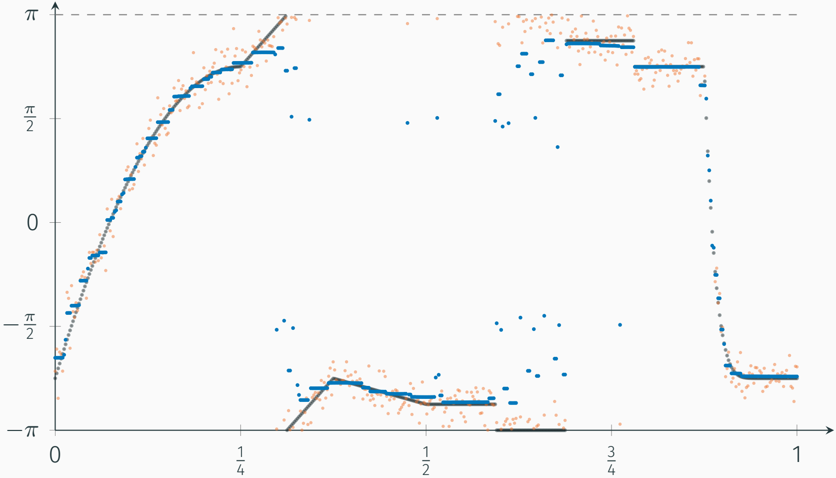

- Comparison of f_o & f_n width f_R
- Denoised with CPPA and realvalued TV_1, ($\alpha = \frac{3}{4}$, $\beta = 0$)
- Artefacts at the “jumps that are none“ from representation

A Signal of Cyclic Data

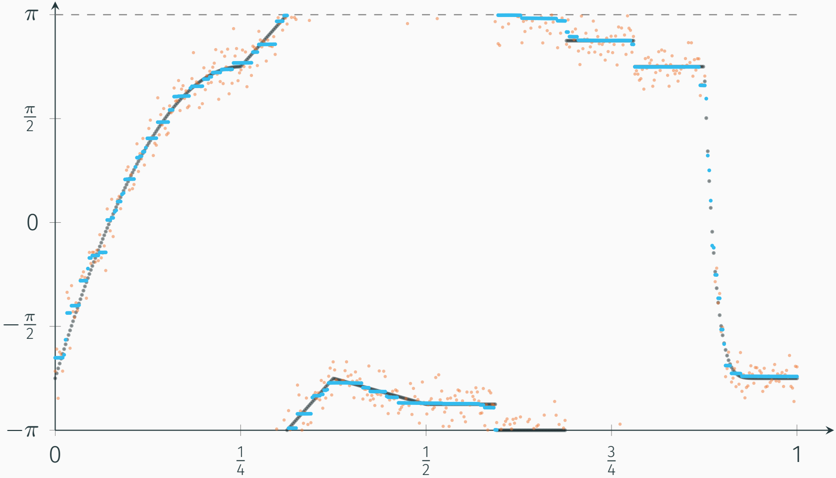

- Comparison of f_{o} & f_{n} width f_1
- Denoised with CPPA and TV_1 $(\alpha = \frac{3}{4}, \beta = 0)$
- but: stair caising

A Signal of Cyclic Data

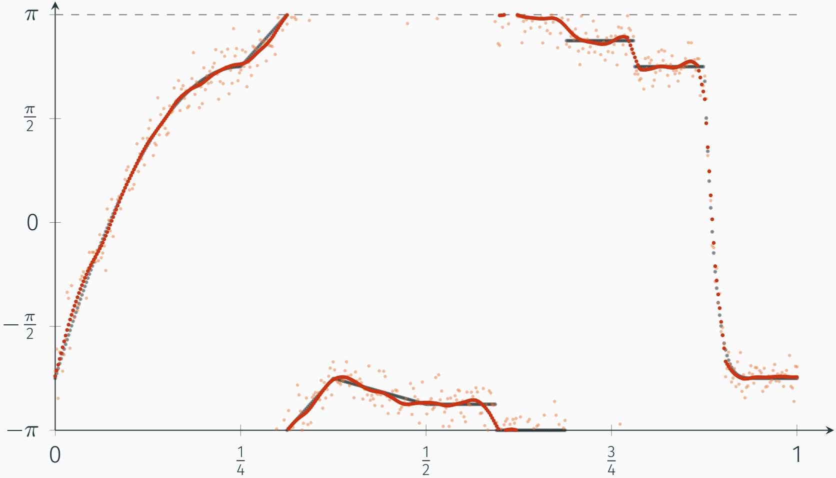

- Comparison of f_o & f_n width f_2
- Denoised with CPPA and TV_2 $(\alpha = 0, \beta = \frac{3}{2})$
- but: problems in constant areas

A Signal of Cyclic Data

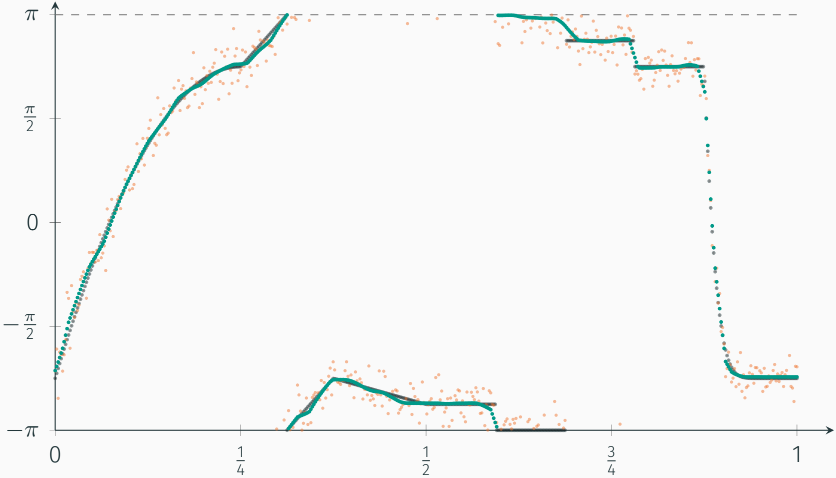

- Comparison of f_o & f_n width f_3
- Denoised with CPPA and $\mathrm{TV}_1\,\&\,\mathrm{TV}_2$ $(\alpha = \frac{1}{4}, \beta = \frac{3}{4})$
- combined: smallest mean squarred error.

Total Variation Regularization

First and Second Order Differences

On $\mathbb{R}^n$

- line $\gamma(t) = x + t(y - x)$
- distance $\|x - y\|_2$
- first order model

$$\sum_{i\in\mathcal{V}} \|f_i - u_i\|_2^2 + \alpha \sum_{i\in\mathcal{G}\setminus\{N\}} \|u_i - u_{i+1}\|_2$$

Riemannian manifold $\mathcal{M}$

- geodesic path $\gamma_{\overset{\frown}{x,y}}(t)$
- geodesic distance $d\colon \mathcal{M} \times \mathcal{M} \to \mathbb{R}$
- first order model

[Strekalovskiy, Cremers, 2011; Lellmann et al., 2013; Weinmann et. al., 2014]

$$\sum_{i\in\mathcal{V}} d(f_i, u_i)^2 + \alpha \sum_{i\in\mathcal{G}\setminus\{N\}} d(u_i, u_{i+1})$$

First and Second Order Differences

On $\mathbb{R}^n$

- line $\gamma(t) = x + t(y-x)$
- distance $\|x-y\|_2$
- first order model

$$\sum_{i\in\mathcal{V}} \|f_i - u_i\|_2^2 + \alpha \sum_{i\in\mathcal{G}\setminus\{N\}} \|u_i - u_{i+1}\|_2$$

- second oder difference

$$\|x - 2y + z\|_2$$

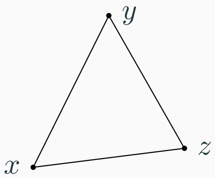

Riemannian manifold $\mathcal{M}$

- geodesic path $\gamma_{\overset{\frown}{x,y}}(t)$
- geodesic distance $d\colon \mathcal{M}\times\mathcal{M}\to\mathbb{R}$
- first order model

[Strekalovskiy, Cremers, 2011; Lellmann et al., 2013; Weinmann et. al., 2014]

$$\sum_{i\in\mathcal{V}} d(f_i, u_i)^2 + \alpha \sum_{i\in\mathcal{G}\setminus\{N\}} d(u_i, u_{i+1})$$

- How to model that on $\mathcal{M}$?

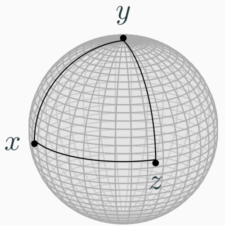

$\mathcal{M} = \mathbb{S}^2$

First and Second Order Differences

On $\mathbb{R}^n$

- line $\gamma(t) = x + t(y - x)$
- distance $\|x - y\|_2$
- first order model

$$\sum_{i\in\mathcal{V}} \|f_i - u_i\|_2^2 + \alpha \sum_{i\in\mathcal{G}\setminus\{N\}} \|u_i - u_{i+1}\|_2$$

- second oder difference

$$2\|\tfrac{1}{2}(x+z) - y\|_2$$

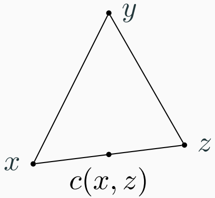

Riemannian manifold $\mathcal{M}$

- geodesic path $\gamma_{\widehat{x,y}}(t)$
- geodesic distance $d\colon \mathcal{M}\times\mathcal{M}\to\mathbb{R}$
- first order model

[Strekalovskiy, Cremers, 2011; Lellmann et al., 2013; Weinmann et. al., 2014]

$$\sum_{i\in\mathcal{V}} d(f_i, u_i)^2 + \alpha \sum_{i\in\mathcal{G}\setminus\{N\}} d(u_i, u_{i+1})$$

- idea: mid point formulation

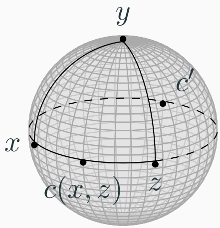

$\mathcal{M} = \mathbb{S}^2$

First and Second Order Differences

On $\mathbb{R}^n$

- line $\gamma(t) = x + t(y - x)$
- distance $\|x - y\|_2$
- first order model

$$\sum_{i\in\mathcal{V}} \|f_i - u_i\|_2^2 + \alpha \sum_{i\in\mathcal{G}\setminus\{N\}} \|u_i - u_{i+1}\|_2$$

- second oder difference

$$2\|c(x,z) - y\|_2$$

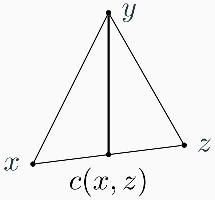

Riemannian manifold $\mathcal{M}$

- geodesic path $\gamma_{\widehat{x,y}}(t)$
- geodesic distance $d\colon \mathcal{M} \times \mathcal{M} \to \mathbb{R}$
- first order model

[Strekalovskiy, Cremers, 2011; Lellmann et al., 2013; Weinmann et. al., 2014]

$$\sum_{i\in\mathcal{V}} d(f_i, u_i)^2 + \alpha \sum_{i\in\mathcal{G}\setminus\{N\}} d(u_i, u_{i+1})$$

- idea: mid point formulation

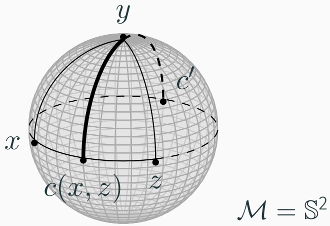

A Second Order TV-type Model

Mid points between $x, z \in \mathcal{M}$:

$\mathcal{C}_{x,z} \coloneqq \{c \in \mathcal{M} : c = \gamma_{\overset{\frown}{x,z}}(\frac{1}{2})$ for any geodesic $\gamma_{\overset{\frown}{x,z}} : [0,1] \to \mathcal{M}\}$

The Absolute Second Order Difference:

$$d_2(x,y,z) \coloneqq \min_{c \in \mathcal{C}_{x,z}} d(c,y), \qquad x,y,z \in \mathcal{M}.$$

$\Rightarrow$ Second Order TV-type Model for $\mathcal{M}$-valued signals f

$$\mathcal{E}(u) \coloneqq \sum_{i \in \mathcal{V}} d(f_i, u_i)^2 + \alpha \sum_{i \in \mathcal{G}\setminus\{N\}} d(u_i, u_{i+1}) + \beta \sum_{i \in \mathcal{G}\setminus\{1,N\}} d_2(u_{i-1}, u_i, u_{i+1})$$

A Second Order TV-type Model

Mid points between $x, z \in \mathcal{M}$:

$\mathcal{C}_{x,z} \coloneqq \left\{c \in \mathcal{M} : c = \gamma_{\overset{\frown}{x,z}}\left(\frac{1}{2}\right) \text{ for any geodesic } \gamma_{\overset{\frown}{x,z}} : [0,1] \to \mathcal{M}\right\}$

The Absolute Second Order Difference:

$$d_2(x,y,z) \coloneqq \min_{c \in \mathcal{C}_{x,z}} d(c,y), \qquad x,y,z \in \mathcal{M}.$$

$\Rightarrow$ Second Order TV-type Model for $\mathcal{M}$-valued signals f

$$\mathcal{E}(u) \coloneqq \sum_{i \in \mathcal{V}} d(f_i,u_i)^2 + \alpha \sum_{i \in \mathcal{G}\setminus\{N\}} d(u_i,u_{i+1}) + \beta \sum_{i \in \mathcal{G}\setminus\{1,N\}} d_2(u_{i-1},u_i,u_{i+1})$$

For images additionally: use $\|w - x + y - z\|_2 = 2\|\frac{1}{2}(w+y) - \frac{1}{2}(x+z)\|_2$ for Absolute Second Order Mixed Difference

$$d_{1,1}(w,x,y,z) \coloneqq \min_{c \in \mathcal{C}_{w,y}, \tilde{c} \in \mathcal{C}_{x,z}} d(c,\tilde{c}), \qquad w,x,y,z \in \mathcal{M}.$$

Proximal Map

For $\varphi\colon \mathcal{M}^n \to (-\infty, +\infty]$ and $\lambda > 0$ we define the Proximal Map as [Moreau, 1965; Rockafellar, 1976; Ferreira, Oliveira, 2002]

$$\operatorname{prox}_{\lambda\varphi}(g) \coloneqq \operatorname*{arg\,min}_{u\in\mathcal{M}^n} \frac{1}{2}\sum_{i=1}^{n} d(u_i, g_i)^2 + \lambda\varphi(u).$$

! For a Minimizer u^* of φ we have $\operatorname{prox}_{\lambda\varphi}(u^*) = u^*$.

- For $\varphi\colon \mathbb{R}^n \to \mathbb{R}$ proper, convex, lower semicontinuous:
  - prox unique.
  - PPA $x_k = \operatorname{prox}_{\lambda\varphi}(x_{k-1})$ converges to $\operatorname{arg\,min}\varphi$
- For $\varphi = \mathcal{E}$ not that useful

The Cyclic Proximal Point Algorithm

For $\varphi = \sum_{l=1}^{c} \varphi_l$ the

Cyclic Proximal Point-Algorithmus (CPPA) reads [Bertsekas, 2011; Bačák, 2014]

$$x^{(k+\frac{l+1}{c})} = \operatorname{prox}_{\lambda_k \varphi_l}(x^{(k+\frac{l}{c})}), \quad l = 0, \ldots, c-1,\ k = 0, 1, \ldots$$

On a Hadamard manifold $\mathcal{M}$:

convergence to a minimizer of φ if

- all φ_l proper, convex, lower semicontinuous
- $\{\lambda_k\}_{k\in\mathbb{N}} \in \ell_2(\mathbb{N})\backslash\ell_1(\mathbb{N})$.

Ansatz.

- efficient Proximal Maps for every summand of $\mathcal{E}(u)$.
- speed up by parallelization

Proximal Maps for Distance and TV summands

Let $\gamma_{\overset{\frown}{x,y}}\colon [0,1] \to \mathcal{M}$ be a geodesic between $x, y \in \mathcal{M}$.

Theorem (Distance term) **[Oliveira, Ferreira, 2002]**
For $\varphi(x) = d^2(x, f)$ with fixed $f \in \mathcal{M}$ we have

$$\operatorname{prox}_{\lambda\varphi}(x) = \gamma_{\overset{\frown}{x,f}}\Bigl(\frac{\lambda d(x,f)}{1 + \lambda d(x,f)}\Bigr)$$

Theorem (First Order Difference Term) **[Weinmann, Storath, Demaret, 2014]**
For $\varphi(x,y) = d(x,y)$ we have

$$\operatorname{prox}_{\lambda\varphi}(x,y) = \bigl(\gamma_{\overset{\frown}{x,y}}(t), \gamma_{\overset{\frown}{x,y}}(1-t)\bigr)$$

with

$$t = \begin{cases} \frac{\lambda}{d(x,y)} & \text{if } \lambda < \frac{1}{2}d(x,y) \\ \frac{1}{2} & \text{else.} \end{cases}$$

Proximal Map for the TV_2 Summand

To compute

$$\operatorname{prox}_{\lambda d_2}(g) = \operatorname*{arg\,min}_{u\in\mathcal{M}^3}\Bigl\{\frac{1}{2}\sum_{i=1}^{3} d(u_i,g_i)^2 + \lambda d_2(u_1,u_2,u_3)\Bigr\}$$

We have

- a closed form solution for $\mathcal{M} = \mathbb{S}^1$
- use a sub gradient descent (as inner problem) with

$$\nabla_{\mathcal{M}^3} d_2 = \bigl(\nabla_{\mathcal{M}} d_2(\cdot,y,z), \nabla_{\mathcal{M}} d_2(x,\cdot,z), \nabla_{\mathcal{M}} d_2(x,y,\cdot)\bigr)^{\mathrm{T}}.$$

where

- $\nabla_{\mathcal{M}} d_2(x,\cdot,z)(y) = -\dfrac{\log_y c(x,z)}{\lVert\log_y c(x,z)\rVert_y} \in T_y\mathcal{M}$
- $\nabla_{\mathcal{M}} d_2(\cdot,y,z)$ and analogously $\nabla_{\mathcal{M}} d_2(\cdot,y,z)$ using Jacobi fields and a chain rule [Bačák, RB, Weinmann, Steidl, 2016]

Bernoulli's Lemniscate on the sphere $\mathbb{S}^2$

$$\gamma(t) \coloneqq \frac{a\sqrt{2}}{\sin^2(t)+1}\bigl(\cos(t), \cos(t)\sin(t), 1\bigr)^{\mathrm{T}}, \quad t \in [0, 2\pi], a = \frac{\pi}{2\sqrt{2}}.$$

Generate a sphere-valued signal by

$$\gamma_S(t) = \exp_p(\gamma(t)), p = (0,0,1)^{\mathrm{T}}$$

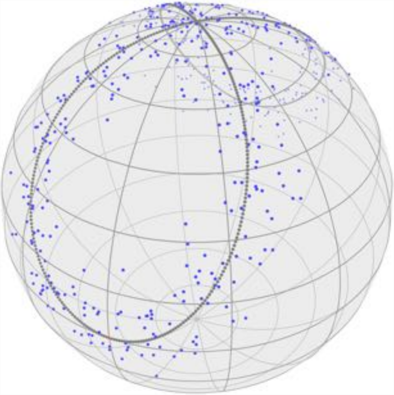

noisy lemniscate of Bernoulli on $\mathbb{S}^2$, Gaussian noise, $\sigma = \frac{\pi}{30}$, on $T_p\mathbb{S}^2$.

Bernoulli's Lemniscate on the sphere $\mathbb{S}^2$

$$\gamma(t) := \frac{a\sqrt{2}}{\sin^2(t)+1}\big(\cos(t), \cos(t)\sin(t), 1\big)^{\mathrm{T}}, \quad t \in [0, 2\pi], a = \frac{\pi}{2\sqrt{2}}.$$

Generate a sphere-valued signal by

$$\gamma_S(t) = \exp_p(\gamma(t)), p = (0,0,1)^{\mathrm{T}}$$

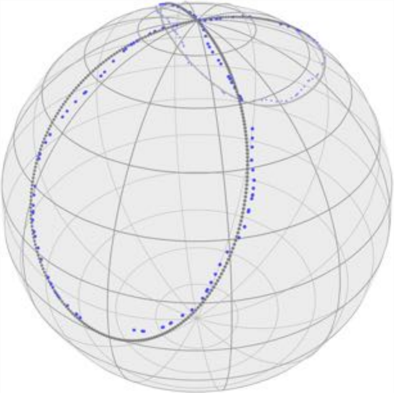

reconstruction with TV_1, $\alpha = 0.21$, $\mathrm{MAE} = 4.08 \times 10^{-2}$.

Bernoulli's Lemniscate on the sphere $\mathbb{S}^2$

$$\gamma(t) \coloneqq \frac{a\sqrt{2}}{\sin^2(t)+1}\big(\cos(t), \cos(t)\sin(t), 1\big)^{\mathrm{T}}, \quad t \in [0, 2\pi], a = \frac{\pi}{2\sqrt{2}}.$$

Generate a sphere-valued signal by

$$\gamma_S(t) = \exp_p(\gamma(t)), p = (0,0,1)^{\mathrm{T}}$$

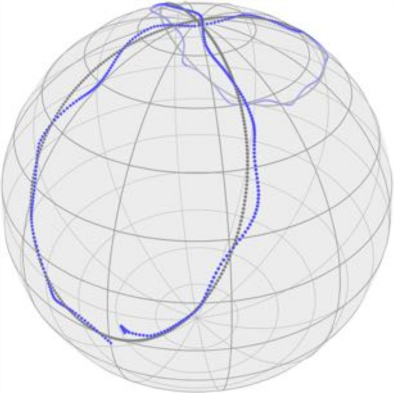

reconstruction with TV_2, $\alpha = 0$, $\beta = 10$, $\mathrm{MAE} = 3.66 \times 10^{-2}$.

Bernoulli's Lemniscate on the sphere $\mathbb{S}^2$

$$\gamma(t) \coloneqq \frac{a\sqrt{2}}{\sin^2(t)+1}\big(\cos(t), \cos(t)\sin(t), 1\big)^{\mathrm{T}}, \quad t \in [0, 2\pi], a = \frac{\pi}{2\sqrt{2}}.$$

Generate a sphere-valued signal by

$$\gamma_S(t) = \exp_p(\gamma(t)), p = (0,0,1)^{\mathrm{T}}$$

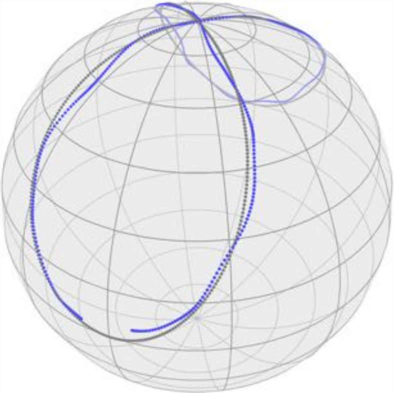

reconstruction with TV_1 & TV_2, $\alpha = 0.16$, $\beta = 12.4$, MAE $= 3.27 \times 10^{-2}$.

Inpainting of $\mathcal{P}(3)$-valued Images

Draw symmetric positive definite 3×3 matrices as ellipsoids

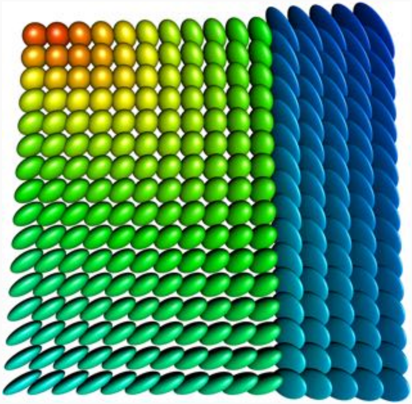

original data

Inpainting of $\mathcal{P}(3)$-valued Images

Draw symmetric positive definite 3×3 matrices as ellipsoids

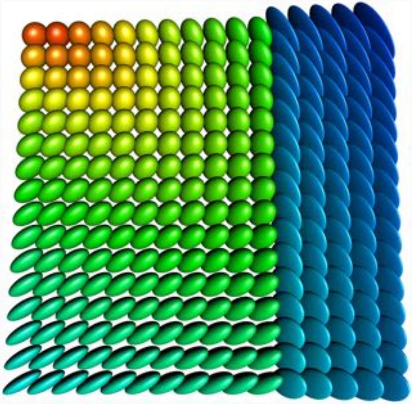

original data

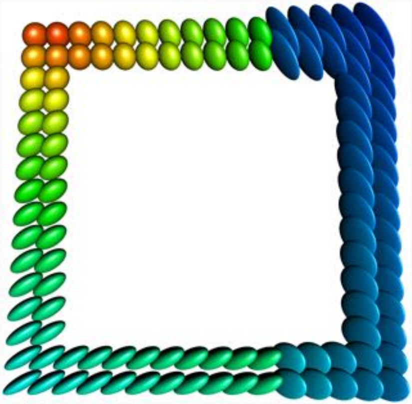

lost (a lot of) data

Inpainting of $\mathcal{P}(3)$-valued Images

Draw symmetric positive definite 3×3 matrices as ellipsoids

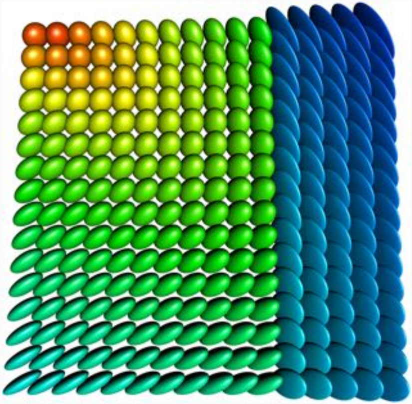

original data

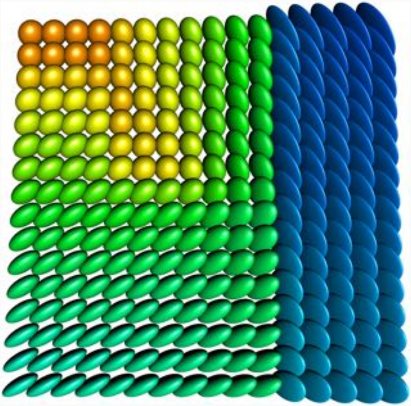

inpainted with $\alpha = \beta = 0.05$,

$\text{MAE} = 0.0929$

Inpainting of $\mathcal{P}(3)$-valued Images

Draw symmetric positive definite 3×3 matrices as ellipsoids

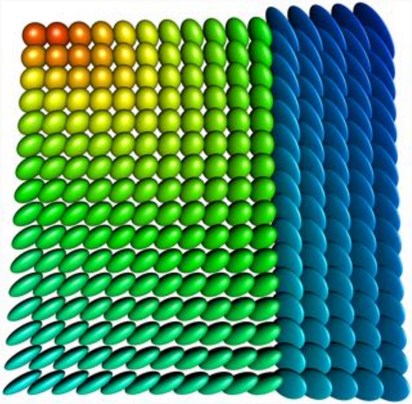

original data

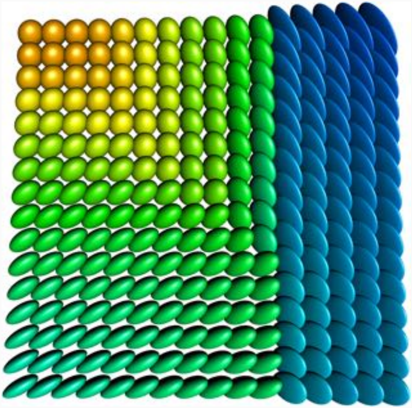

inpainted with $\alpha = 0.1$,

$\text{MAE} = 0.0712$

Properties and Improvements I

The cyclic proximal point algorithm is

- highly parallelizable
- very flexible
- known to converge (arbitrarily) slow

Improvements for first order TV

- parallel Douglas-Rachford algorithm: [RB, Persch, Steidl, 2016]
  only on Hadamard manifolds, faster convergence observed
- half-quadratic minimization: [RB, Chan, Hielscher, Persch, Steidl, 2016]
  relaxation and gradient descent or quasi-Newton.

Instead of addition: infimal convolution, let $\beta \in [0,1]$ be given and

$$\mathcal{R}(u) = \inf_{u=v+w} \beta\mathrm{TV}(v) + (1-\beta)\mathrm{TV}_2(w)$$

or similarly total generalized variation (TGV).

The question is again

What is "$+$" on a manifold?

[RB,Fitschen,Persch,Steid, 2018; Bredies, Holler, Storath, Weinmann, 2018]

Or to phrase the question a little more formal

What are the core properties of the regulariser to keep?

Properties and Improvements II

Instead of addition: infimal convolution, let $\beta \in [0,1]$ be given and

$$\mathcal{R}(u) = \inf_{w} \beta \mathrm{TV}(u-w) + (1-\beta)\mathrm{TV}_2(w)$$

or similarly total generalized variation (TGV).

The question is again

What is "$-$" on a manifold?

[RB,Fitschen,Persch,Steid, 2018; Bredies, Holler, Storath, Weinmann, 2018]

Or to phrase the question a little more formal

What are the core properties of the regulariser to keep?

The Graph p-Laplacian

Finite Weighted Graphs for Image Processing

A pixel might have a...

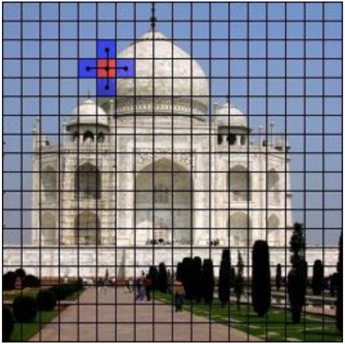

Local neighborhood

Finite Weighted Graphs for Image Processing

A pixel might have a…

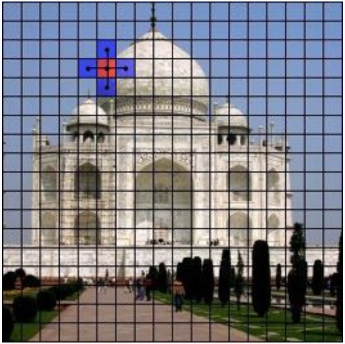

Local neighborhood

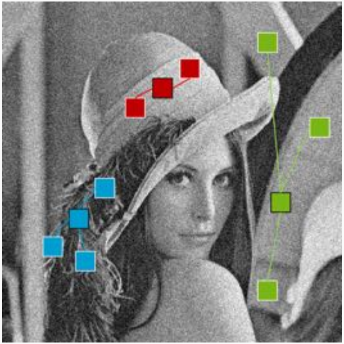

Nonlocal neighborhood

Finite Weighted Graphs for Image Processing

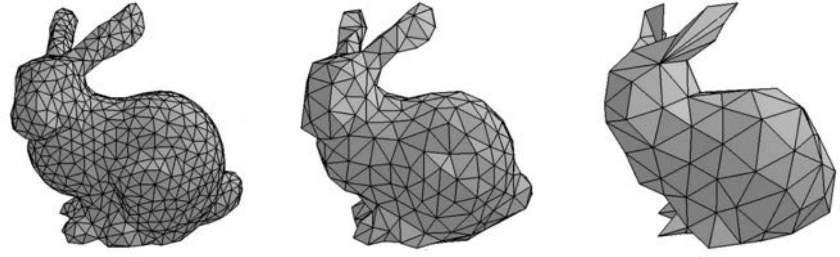

Polygon mesh approximation of a 3D surface. Image courtesy: Gabriel Peyré

"...Everything can be modeled as a graph"

The Graph Framework I

Let $G = (V, E, w)$ be a weighted (directed) graph, i.e.,

- V a finite set of nodes
- $E \subset V \times V$ a finite set of edges $(u, v) \in E$ short: $v \sim u$
- $w \colon V \times V \to \mathbb{R}^+$ a weight function with: $w(u, v) > 0 \Leftrightarrow (u, v) \in E$

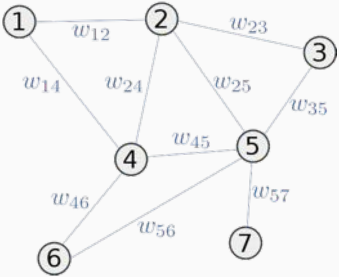

The Graph Framework II

Aim: Notion of a finite difference for data of arbitrary topology

[Almoataz, Lézoray, Bougleux, 2008]

$$\nabla f(u,v) = \sqrt{w(u,v)}\,\big(f(v) - f(u)\big)$$

Special case: Finite differences

Let $G = (V, E, w)$ be a directed 2-neighbour grid graph with the weight function w chosen as:

$$w(u,v) = \begin{cases} \frac{1}{h^2}\,, & \text{if } u \sim v \\ 0\,, & \text{else} \end{cases}$$

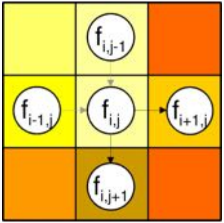

Translating Higher Order Differential Operators

Idea: Mimic important PDEs from image processing on finite weighted graphs, e.g., the p-Laplacian equation

[Elmoataz, Toutain, Tenbrinck, 2015]

Translating Higher Order Differential Operators

Idea: Mimic important PDEs from image processing on finite weighted graphs, e.g., the p-Laplacian equation

[Elmoataz, Toutain, Tenbrinck, 2015]

Let $\Omega \subset \mathbb{R}^n$ an open, bounded set, let $1 \leq p < \infty$ and $f : \Omega \to \mathbb{R}^m$. We are interested in a solution of the homogeneous p-Laplace equation

$$\begin{aligned} \Delta_p f(x) &= -\operatorname{div}\left(\left\|\frac{\partial f}{\partial x_i}\right\|^{p-2} \frac{\partial f}{\partial x_i}\right)(x) \\ &= -\sum_{i=1}^{n}\left(\frac{\partial}{\partial x_i}\left\|\frac{\partial f}{\partial x_i}\right\|^{p-2} \frac{\partial f}{\partial x_i}\right)(x) = 0 \end{aligned}$$

Translating Higher Order Differential Operators

Idea: Mimic important PDEs from image processing on finite weighted graphs, e.g., the p-Laplacian equation

[Elmoataz, Toutain, Tenbrinck, 2015]

Let $G(V, E, w)$ a finite weighted graph, let $1 \leq p < \infty$ and $f : V \to \mathbb{R}^m$ a vertex function. We are interested in a solution of the following finite difference equation:

$$
\begin{aligned}
\Delta_{w,p} f(u) &= \frac{1}{2} \operatorname{div} \left(\|\nabla f\|^{p-2} \nabla f \right)(u) \\
&= -\sum_{v \sim u} (w(u,v))^{p/2} \|f(v) - f(u)\|^{p-2} (f(v) - f(u)) = 0
\end{aligned}
$$

Translating Higher Order Differential Operators

Idea: Mimic important PDEs from image processing on finite weighted graphs, e.g., the p-Laplacian equation

[Elmoataz, Toutain, Tenbrinck, 2015]

Let $G(V, E, w)$ a finite weighted graph, let $1 \leq p < \infty$ and $f: V \to \mathbb{R}^m$ a vertex function. We are interested in a solution of the following finite difference equation:

$$\begin{aligned} \Delta_{w,p} f(u) &= \frac{1}{2} \operatorname{div} \left(\|\nabla f\|^{p-2} \nabla f \right)(u) \\ &= -\sum_{v \sim u} (w(u,v))^{p/2} \|f(v) - f(u)\|^{p-2} (f(v) - f(u)) = 0 \end{aligned}$$

Can we do the same for
manifold-valued vertex functions $f: V \to \mathcal{M}$?

The Basic Idea

On $\mathbb{R}^n$

$$\mathcal{H}(V;\mathbb{R}^m) = \{f\colon V \to \mathbb{R}^m\}$$

Space of edge functions

$$\mathcal{H}(E;\mathbb{R}^m) = \{H\colon E \to \mathbb{R}^m, \\ H(u,v) \in \mathbb{R}^m, (u,v) \in E\}$$

Gradient

$$\nabla f(u,v) \\ = \sqrt{w(u,v)}\big(f(v) - f(u)\big)$$

Local variation

$$\|\nabla f\|^p_{p,f(u)} \\ = \sum_{v\sim u} \sqrt{w(u,v)}^p \, \|f(v) - f(u)\|^p$$

The Basic Idea

On $\mathbb{R}^n$

$$\mathcal{H}(V;\mathbb{R}^m) = \{f\colon V \to \mathbb{R}^m\}$$

Riemannian Manifold $\mathcal{M}$

$$\mathcal{H}(V;\mathcal{M}) := \{f\colon V \to \mathcal{M}\}$$

Space of edge functions

$$\mathcal{H}(E;\mathbb{R}^m) = \{H\colon E \to \mathbb{R}^m,\\ H(u,v) \in \mathbb{R}^m, (u,v) \in E\}$$

$$\mathcal{H}(E;T_f\mathcal{M}) = \{H_f\colon E \to \mathrm{T}\mathcal{M},\\ H_f(u,v) \to \mathrm{T}_{f(u)}\mathcal{M}, (u,v) \in E\}$$

Gradient

$$\nabla f(u,v)\\ = \sqrt{w(u,v)}\big(f(v) - f(u)\big)$$

Local variation

$$\|\nabla f\|^p_{p,f(u)}\\ = \sum_{v\sim u} \sqrt{w(u,v)}^p \, \|f(v) - f(u)\|^p$$

The Basic Idea

On $\mathbb{R}^n$

$$\mathcal{H}(V;\mathbb{R}^m) = \{f\colon V \to \mathbb{R}^m\}$$

Riemannian Manifold $\mathcal{M}$

$$\mathcal{H}(V;\mathcal{M}) \coloneqq \{f\colon V \to \mathcal{M}\}$$

Space of edge functions

$$\mathcal{H}(E;\mathbb{R}^m) = \{H\colon E \to \mathbb{R}^m, \quad H(u,v) \in \mathbb{R}^m, (u,v) \in E\}$$

$$\mathcal{H}(E;T_f\mathcal{M}) = \{H_f\colon E \to \mathrm{T}\mathcal{M}, \quad H_f(u,v) \to \mathrm{T}_{f(u)}\mathcal{M}, (u,v) \in E\}$$

Gradient

$$\nabla f(u,v) = \sqrt{w(u,v)}\big(f(v) - f(u)\big)$$

$$\nabla f(u,v) \coloneqq \sqrt{w(u,v)} \log_{f(u)} f(v) \in T_{f(u)}\mathcal{M}$$

Local variation

$$\|\nabla f\|^p_{p,f(u)} = \sum_{v\sim u} \sqrt{w(u,v)}^p \, \|f(v) - f(u)\|^p$$

The Basic Idea

On $\mathbb{R}^n$

$$\mathcal{H}(V;\mathbb{R}^m) = \{f\colon V \to \mathbb{R}^m\}$$

Riemannian Manifold $\mathcal{M}$

$$\mathcal{H}(V;\mathcal{M}) := \{f\colon V \to \mathcal{M}\}$$

Space of edge functions

$$\mathcal{H}(E;\mathbb{R}^m) = \{H\colon E \to \mathbb{R}^m,\ H(u,v) \in \mathbb{R}^m, (u,v) \in E\}$$

$$\mathcal{H}(E;T_f\mathcal{M}) = \{H_f\colon E \to \mathrm{T}\mathcal{M},\ H_f(u,v) \to \mathrm{T}_{f(u)}\mathcal{M}, (u,v) \in E\}$$

Gradient

$$\nabla f(u,v) = \sqrt{w(u,v)}\big(f(v) - f(u)\big)$$

$$\nabla f(u,v) := \sqrt{w(u,v)}\log_{f(u)} f(v) \in T_{f(u)}\mathcal{M}$$

Local variation

$$\|\nabla f\|^p_{p,f(u)} = \sum_{v\sim u} \sqrt{w(u,v)}^p \, \|f(v) - f(u)\|^p$$

$$\|\nabla f\|^p_{p,f(u)} := \sum_{v\sim u} \sqrt{w(u,v)}^p d_{\mathcal{M}}(f(u),f(v))^p$$

(Local) Divergence

What is $\langle \nabla f, H \rangle = \langle f, \nabla^\star H \rangle$, $\nabla^\star = -\operatorname{div}$, on a manifold?

(Local) Divergence

Theorem [RB, Tenbrinck, 2018]
For $f \in \mathcal{H}(V;\mathcal{M})$, $H_f \in \mathcal{H}(E;\mathrm{T}_f\mathcal{M})$, we have

$$\langle \nabla f, H_f \rangle_{\mathcal{H}(E;\mathrm{T}_f\mathcal{M})} = \sum_{u\in V}\sum_{v\sim u} \langle \log_{f(u)} f(v), -\operatorname{div} H_f(u) \rangle_{f(u)},$$

where the local divergence is given by

$$\operatorname{div} H_f(u) := \frac{1}{2}\sum_{v\sim u} \sqrt{w(v,u)}\,\mathrm{PT}_{f(v)\to f(u)} H_f(v,u) - \sqrt{w(u,v)} H_f(u,v)$$

(Local) Divergence

Theorem [RB, Tenbrinck, 2018]
For $f \in \mathcal{H}(V;\mathcal{M})$, $H_f \in \mathcal{H}(E;\mathrm{T}_f\mathcal{M})$, we have

$$\langle \nabla f, H_f \rangle_{\mathcal{H}(E;\mathrm{T}_f\mathcal{M})} = \sum_{u\in V}\sum_{v\sim u}\langle \log_{f(u)} f(v), -\operatorname{div} H_f(u)\rangle_{f(u)},$$

where the local divergence is given by

$$\operatorname{div} H_f(u) := \frac{1}{2}\sum_{v\sim u}\sqrt{w(v,u)}\,\mathrm{PT}_{f(v)\to f(u)}\, H_f(v,u) - \sqrt{w(u,v)}H_f(u,v)$$

Remark
By antisymmetry $\nabla f(u,v) = -\mathrm{PT}_{f(v)\to f(u)}\,\nabla f(v,u) \in \mathrm{T}_{f(u)}\mathcal{M}$
we get

$$\operatorname{div}(\nabla f)(u) = -\sum_{v\sim u} w(u,v)\log_{f(u)} f(v)$$

The Manifold-valued Graph p-Laplacians

We define the Graph p-Laplacians:

- anisotropic $\Delta_p^{\mathrm{a}} \colon \mathcal{H}(V;\mathcal{M}) \to \mathcal{H}(V;T\mathcal{M})$ by

$$\begin{aligned}\Delta_p^{\mathrm{a}} f(u) &:= \operatorname{div}\bigl(\lVert\nabla f\rVert_{f(\cdot)}^{p-2}\,\nabla f\bigr)(u)\\ &= -\sum_{v\sim u}\sqrt{w(u,v)}^{p}\,d_{\mathcal{M}}^{p-2}(f(u),f(v))\log_{f(u)} f(v)\end{aligned}$$

- isotropic $\Delta_p^{\mathrm{i}} \colon \mathcal{H}(V;\mathcal{M}) \to \mathcal{H}(V;T\mathcal{M})$ by

$$\begin{aligned}\Delta_p^{\mathrm{i}} f(u) &:= \operatorname{div}\bigl(\lVert\nabla f\rVert_{2,f(\cdot)}^{p-2}\nabla f\bigr)(u)\\ &= -\,b_{\mathrm{i}}(u)\sum_{v\sim u} w(u,v)\log_{f(u)} f(v)\ ,\end{aligned}$$

where

$$b_{\mathrm{i}}(u) := \lVert\nabla f\rVert_{2,f(u)}^{p-2} = \Bigl(\sum_{v\sim u} w(u,v)\,d_{\mathcal{M}}^{2}(f(u),f(v))\Bigr)^{\frac{p-2}{2}}.$$

Variational Optimization Problems

Goal: A Minimizer of a variational model $\mathcal{E}\colon \mathcal{H}(V;\mathcal{M}) \to \mathbb{R}$

the anisotropic energy functional

[Lellmann, Strekalovskiy, Kötters, Cremers, '13; Weinmann, Demaret, Storath, '14; RB, Persch, Steidl, '16]

$$\mathcal{E}_{\mathrm{a}}(f) \ := \frac{\lambda}{2} \sum_{u \in V} d^2_{\mathcal{M}}(f_0(u), f(u)) \ + \ \frac{1}{p} \sum_{(u,v) \in E} \lVert \nabla f(u,v) \rVert^p_{f(u)},$$

and the isotropic energy functional

[RB, Chan, Hielscher, Persch, Steidl, '16; RB, Fitschen, Persch, Steidl, '18]

$$\mathcal{E}_{\mathrm{i}}(f) \ := \frac{\lambda}{2} \sum_{u \in V} d^2_{\mathcal{M}}(f_0(u), f(u)) \ + \ \frac{1}{p} \sum_{u \in V} \Bigl(\sum_{v \sim u} \lVert \nabla f(u,v) \rVert^2_{f(u)} \Bigr)^{p/2}.$$

Optimality Conditions

For $e \in \{\mathrm{a},\mathrm{i}\}$ and any $u \in V$ we have for a minimizer

$$0 \overset{!}{=} \Delta_p^e f(u) - \lambda \log_{f(u)} f_0(u) \in \mathrm{T}_{f(u)}\mathcal{M}.$$

Optimality Conditions

For $e \in \{\mathrm{a}, \mathrm{i}\}$ and any $u \in V$ we have for a minimizer

$$0 \overset{!}{=} \Delta_p^e f(u) - \lambda \log_{f(u)} f_0(u) \in \mathrm{T}_{f(u)}\mathcal{M}.$$

Algorithm I. Forward difference or explicit scheme:

$$f_{n+1}(u) = \exp_{f_n(u)}\bigl(\Delta t\,(\Delta_p^{\mathrm{e}} f_n(u) - \lambda \log_{f_n(u)} f_0(u))\bigr)$$

! to meet CFL conditions: small Δt necessary

Optimality Conditions

For $e \in \{\mathrm{a}, \mathrm{i}\}$ and any $u \in V$ we have for a minimizer

$$0 \overset{!}{=} \Delta_p^e f(u) - \lambda \log_{f(u)} f_0(u) \in \mathrm{T}_{f(u)}\mathcal{M}.$$

Algorithm I. Forward difference or explicit scheme:

$$f_{n+1}(u) = \exp_{f_n(u)}\bigl(\Delta t\,(\Delta_p^{\mathrm{e}} f_n(u) - \lambda \log_{f_n(u)} f_0(u))\bigr)$$

! to meet CFL conditions: small Δt necessary

Algorithm II. Jacobi iteration

$$f_{n+1}(u) = \exp_{f_n(u)}\left(\frac{\displaystyle\sum_{v\sim u} b(u,v) \log_{f_n(u)} f_n(v) + \lambda \log_{f_n(u)} f_0(u)}{\displaystyle\lambda + \sum_{v\sim u} b(u,v)}\right),$$

$$b(u,v) = \begin{cases} \sqrt{w(u,v)}^p d_{\mathcal{M}}^{p-2}(f(u), f(v)), & e = \mathrm{a},\\ b_{\mathrm{i}}(u), & e = \mathrm{i}. \end{cases}$$

Evolution of the Graph p-Laplacian

- $\mathcal{M} = \mathbb{S}^2$
- $V = \{1, \ldots, 64\} \times \{1, \ldots, 64\}$ pixel grid
- E is the 4-neighborhood, Neumann boundary

f_0

$\lambda = 0$ (no data term)

Evolution of the Graph p-Laplacian

- $\mathcal{M} = \mathbb{S}^2$
- $V = \{1, \ldots, 64\} \times \{1, \ldots, 64\}$ pixel grid
- E is the 4-neighborhood, Neumann boundary

f_0

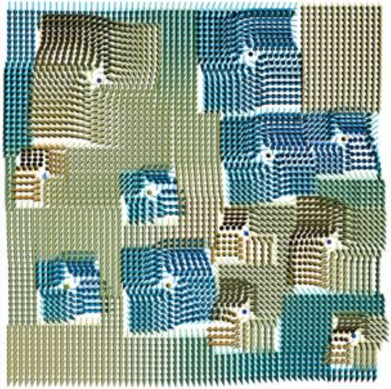

f_{1000}

$\lambda = 0$, $p = 1$, anisotropic

Evolution of the Graph p-Laplacian

- $\mathcal{M} = \mathbb{S}^2$
- $V = \{1, \ldots, 64\} \times \{1, \ldots, 64\}$ pixel grid
- E is the 4-neighborhood, Neumann boundary

f_0

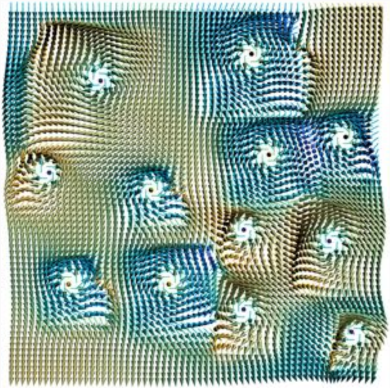

f_{1000}

$\lambda = 0$, $p = 1$, isotropic

Evolution of the Graph p-Laplacian

- $\mathcal{M} = \mathbb{S}^2$
- $V = \{1, \ldots, 64\} \times \{1, \ldots, 64\}$ pixel grid
- E is the 4-neighborhood, Neumann boundary

f_0

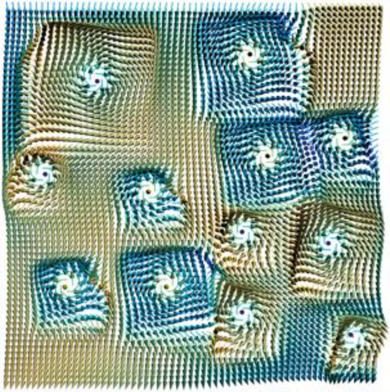

f_{1000}

$\lambda = 0$, $p = 1$, $p = 2$, (an)isotropic

Local Image Denoising

Light Detection and Ranging data (LiDaR), 40×40 pixel

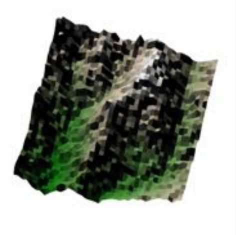

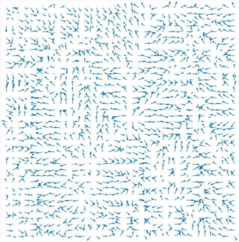

original data

[Geesch et al., 2009] via MFOPT

lellmann.net/software/mfopt

Local Image Denoising

Light Detection and Ranging data (LiDaR), 40×40 pixel

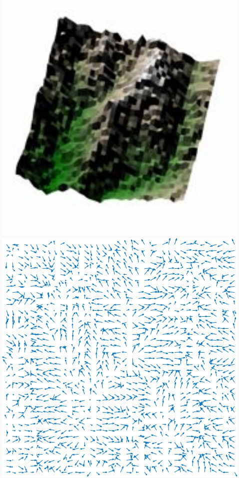

original data

[Geesch et al., 2009] via MFOPT

lellmann.net/software/mfopt

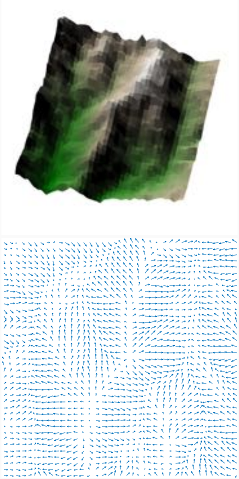

$p = 2$, $\lambda = 0.5$,

(an)isotropic.

Local Image Denoising

Light Detection and Ranging data (LiDaR), 40×40 pixel

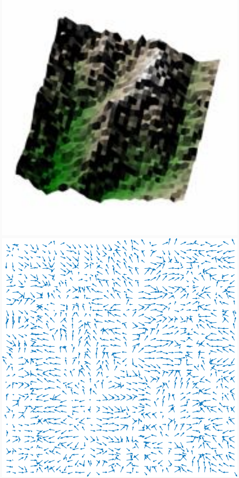

original data

[Geesch et al., 2009] via MFOPT

lellmann.net/software/mfopt

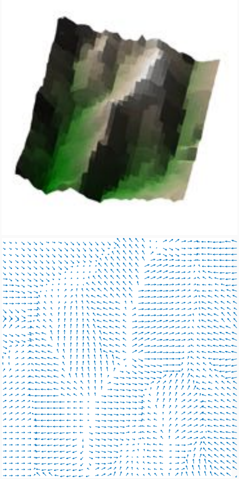

$p = 1$, $\lambda = 2$,

anisotropic.

Local Image Denoising

Light Detection and Ranging data (LiDaR), 40×40 pixel

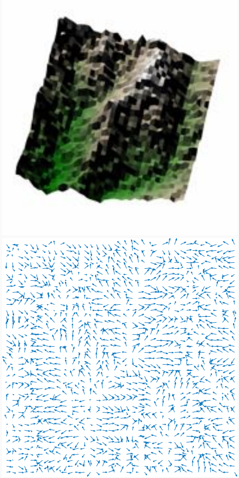

original data

[Geesch et al., 2009] via MFOPT

lellmann.net/software/mfopt

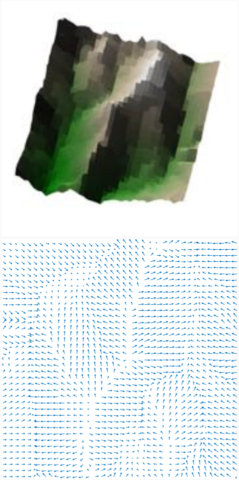

$p = 1, \lambda = 2,$

anisotropic.

$p = 0.1, \lambda = 1,$

anisotropic.

Nonlocal Image Denoising

- $\mathcal{M} = \mathbb{S}^1$, phase in $[-\pi, \pi)$, color: hue
- $V = \{1, \ldots, 256\} \times \{1, \ldots, 256\}$ pixel grid
- E from 12 most similar pixels w.r.t. 17×17 patch distances

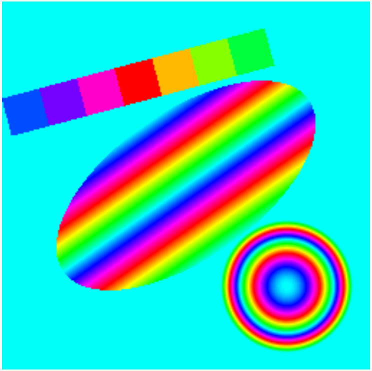

original.

Nonlocal Image Denoising

- $\mathcal{M} = \mathbb{S}^1$, phase in $[-\pi, \pi)$, color: hue
- $V = \{1, \ldots, 256\} \times \{1, \ldots, 256\}$ pixel grid
- E from 12 most similar pixels w.r.t. 17×17 patch distances

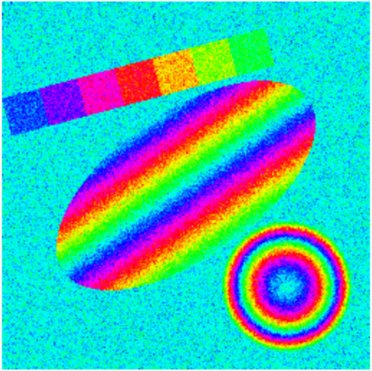

wrapped Gaussian, $\sigma = 0.3$.

Nonlocal Image Denoising

- $\mathcal{M} = \mathbb{S}^1$, phase in $[-\pi, \pi)$, color: hue
- $V = \{1, \ldots, 256\} \times \{1, \ldots, 256\}$ pixel grid
- E from 12 most similar pixels w.r.t. 17×17 patch distances

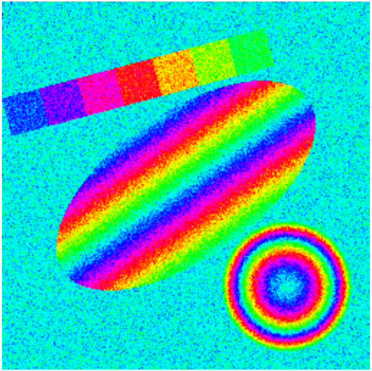

wrapped Gaussian, $\sigma = 0.3$.

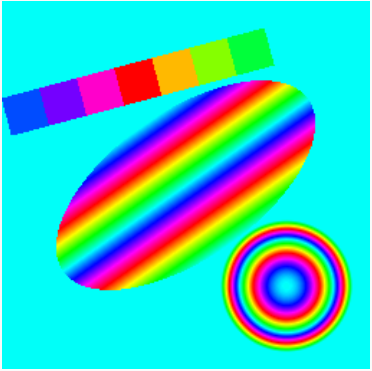

NL-MMSE. [Laus et al., 2017]

$\varepsilon = 2.50 \times 10^{-3}$

Nonlocal Image Denoising

- $\mathcal{M} = \mathbb{S}^1$, phase in $[-\pi, \pi)$, color: hue
- $V = \{1, \ldots, 256\} \times \{1, \ldots, 256\}$ pixel grid
- E from 12 most similar pixels w.r.t. 17×17 patch distances

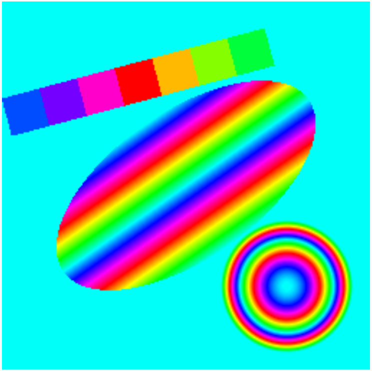

original.

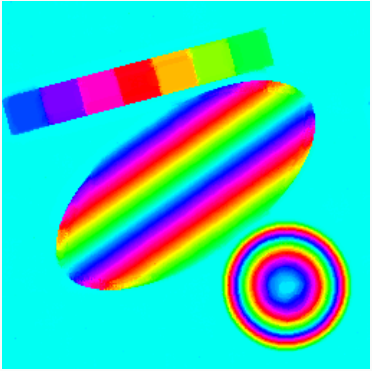

anisotropic, $p = 1$, $\lambda = 2^{-8}$, $\varepsilon = 2.67 \times 10^{-3}$.

Local denoising on a surface

- $\mathcal{M} = \mathcal{P}(3)$
- $V =$ point cloud: boundary of Camino dataset[1]
- local Neighborhood, $d_{\max} = 2$

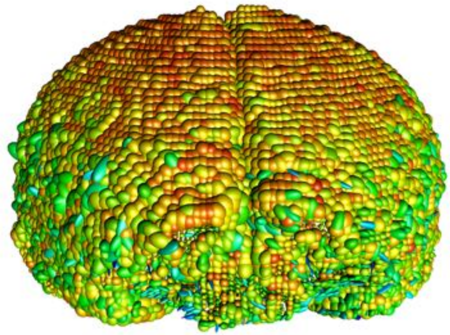

Original Data

[1] Data available from The Camino Project, cmic.cs.ucl.ac.uk/camino

Local denoising on a surface

- $\mathcal{M} = \mathcal{P}(3)$
- V = point cloud: boundary of Camino dataset[1]
- local Neighborhood, $d_{\max} = 2$

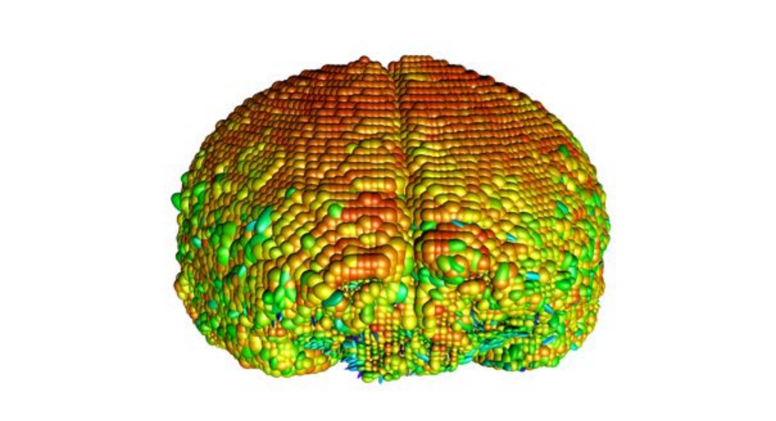

$\lambda = 50$, anisotropic 1-Laplace.

[1] Data available from The Camino Project, cmic.cs.ucl.ac.uk/camino

Summary

We have for manifold valued images $f\colon \mathcal{V} \to \mathcal{M}$

- a model for a first and second order TV-type functional $\mathcal{E}(u)$
- cyclic proximal point algorithm to minimize $\mathcal{E}(u)$
- proof of convergence
- Code available:

ronnybergmann.net/mvirt/

Furthermore manifold valued vertex functions $f\colon V \to \mathcal{M}$

- includes nonlocal methods and data on surfaces
- manifold valued graph p-Laplacian
- Code available soon.

Future work

- different couplings (infimal convolution)
- other algorithms
- different settings, e.g. constraint optimization
- applications to e.g.
  - DT-MRI
  - phase valued data
  - EBSD data
  - other manifolds?
- other image processing tasks
- continuous models

...and an implementation in Julia (work in progress).

References

R. Bergmann and D. Tenbrinck. "A graph framework for manifold-valued data". In: *SIAM Journal on Imaging Sciences* 11 (1 2018), pp. 325–360. arXiv: 1702.05293.

M. Bačák, R. Bergmann, G. Steidl, and A. Weinmann. "A second order non-smooth variational model for restoring manifold-valued images". In: *SIAM Journal on Scientific Computing* 38.1 (2016), A567–A597. arXiv: 1506.02409.

R. Bergmann, J. Persch, and G. Steidl. "A parallel Douglas–Rachford algorithm for minimizing ROF-like functionals on images with values in symmetric Hadamard manifolds". In: *SIAM Journal on Imaging Sciences* 9.3 (2016), pp. 901–937. arXiv: 1512.02814.

R. Bergmann, J. H. Fitschen, J. Persch, and G. Steidl. "Priors with coupled first and second order differences for manifold-valued image processing". In: *Journal of Mathematical Imaging and Vision* (2018). accepted, online first. arXiv: 1709.01343.

Thank you for your attention.

- R. Bergmann and D. Tenbrinck. "A graph framework for manifold-valued data". In: *SIAM Journal on Imaging Sciences* 11 (1 2018), pp. 325–360. arXiv: 1702.05293.
- M. Bačák, R. Bergmann, G. Steidl, and A. Weinmann. "A second order non-smooth variational model for restoring manifold-valued images". In: *SIAM Journal on Scientific Computing* 38.1 (2016), A567–A597. arXiv: 1506.02409.
- R. Bergmann, J. Persch, and G. Steidl. "A parallel Douglas–Rachford algorithm for minimizing ROF-like functionals on images with values in symmetric Hadamard manifolds". In: *SIAM Journal on Imaging Sciences* 9.3 (2016), pp. 901–937. arXiv: 1512.02814.
- R. Bergmann, J. H. Fitschen, J. Persch, and G. Steidl. "Priors with coupled first and second order differences for manifold-valued image processing". In: *Journal of Mathematical Imaging and Vision* (2018). accepted, online first. arXiv: 1709.01343.